

This is a repository copy of *Solving the Puzzles of the Decay of the Heaviest Known Proton-Emitting Nucleus 185Bi*.

White Rose Research Online URL for this paper:  
<https://eprints.whiterose.ac.uk/180337/>

Version: Published Version

---

**Article:**

Doherty, D. T., Andreyev, A. N. [orcid.org/0000-0003-2828-0262](https://orcid.org/0000-0003-2828-0262), Seweryniak, D. et al. (23 more authors) (2021) Solving the Puzzles of the Decay of the Heaviest Known Proton-Emitting Nucleus 185Bi. *Physical Review Letters*. 202501. ISSN 1079-7114

<https://doi.org/10.1103/PhysRevLett.127.202501>

---

**Reuse**

Items deposited in White Rose Research Online are protected by copyright, with all rights reserved unless indicated otherwise. They may be downloaded and/or printed for private study, or other acts as permitted by national copyright laws. The publisher or other rights holders may allow further reproduction and re-use of the full text version. This is indicated by the licence information on the White Rose Research Online record for the item.

**Takedown**

If you consider content in White Rose Research Online to be in breach of UK law, please notify us by emailing [eprints@whiterose.ac.uk](mailto:eprints@whiterose.ac.uk) including the URL of the record and the reason for the withdrawal request.

Solving the Puzzles of the Decay of the Heaviest Known Proton-Emitting Nucleus  $^{185}\text{Bi}$ 

D. T. Doherty<sup>1,2</sup>, A. N. Andreyev<sup>2,3</sup>, D. Seweryniak<sup>4</sup>, P. J. Woods<sup>5</sup>, M. P. Carpenter<sup>4</sup>, K. Auranen<sup>4,\*</sup>,  
 A. D. Ayangeakaa<sup>6,7</sup>, B. B. Back<sup>4</sup>, S. Bottoni<sup>4,†</sup>, L. Canete<sup>1</sup>, J. G. Cubiss<sup>2</sup>, J. Harker<sup>4,8</sup>, T. Haylett<sup>2</sup>, T. Huang<sup>4,9</sup>,  
 R. V. F. Janssens<sup>6,7</sup>, D. G. Jenkins<sup>2</sup>, F. G. Kondev<sup>4</sup>, T. Lauritsen<sup>4</sup>, C. Lederer-Woods<sup>5</sup>, J. Li<sup>4</sup>, C. Müller-Gatermann<sup>4</sup>,  
 D. Potterveld<sup>4</sup>, W. Reviol<sup>4</sup>, G. Savard<sup>4</sup>, S. Stolze<sup>4</sup>, and S. Zhu<sup>4</sup>

<sup>1</sup>Department of Physics, University of Surrey, Guildford GU2 7XH, United Kingdom

<sup>2</sup>Department of Physics, University of York, York YO10 5DD, United Kingdom

<sup>3</sup>Advanced Science Research Center, Japan Atomic Energy Agency, Tokai-Mura, Naka-gun, Ibaraki 319-1195, Japan

<sup>4</sup>Physics Division, Argonne National Laboratory, Argonne, Illinois 60439, USA

<sup>5</sup>Department of Physics and Astronomy, University of Edinburgh, Edinburgh, EH9 3JZ, United Kingdom

<sup>6</sup>Department of Physics, University of North Carolina at Chapel Hill, Chapel Hill, North Carolina 27599, USA

<sup>7</sup>Triangle Universities Nuclear Laboratory, Duke University, Durham, North Carolina 27708, USA

<sup>8</sup>Department of Chemistry and Biochemistry, University of Maryland, College Park, Maryland 20742, USA

<sup>9</sup>CAS Key Laboratory of High Precision Nuclear Spectroscopy, Institute of Modern Physics, Chinese Academy of Sciences, Lanzhou 730000, China

(Received 25 June 2021; revised 1 September 2021; accepted 27 September 2021; published 12 November 2021)

Two long-standing puzzles in the decay of  $^{185}\text{Bi}$ , the heaviest known proton-emitting nucleus are revisited. These are the nonobservation of the  $9/2^-$  state, which is the ground state of all heavier odd- $A$  Bi isotopes, and the hindered nature of proton and  $\alpha$  decays of its presumed  $60\text{-}\mu\text{s}$   $1/2^+$  ground state. The  $^{185}\text{Bi}$  nucleus has now been studied with the  $^{95}\text{Mo}(^{93}\text{Nb}, 3n)$  reaction in complementary experiments using the Fragment Mass Analyzer and Argonne Gas-Filled Analyzer at Argonne National Laboratory's ATLAS facility. The experiments have established the existence of two states in  $^{185}\text{Bi}$ ; the short-lived  $T_{1/2} = 2.8_{-1.0}^{+2.3}$   $\mu\text{s}$ , proton- and  $\alpha$ -decaying ground state, and a  $58(2)\text{-}\mu\text{s}$   $\gamma$ -decaying isomer, the half-life of which was previously attributed to the ground state. The reassignment of the ground-state lifetime results in a proton-decay spectroscopic factor close to unity and represents the only known example of a ground-state proton decay to a daughter nucleus ( $^{184}\text{Pb}$ ) with a major shell closure. The data also demonstrate that the ordering of low- and high-spin states in  $^{185}\text{Bi}$  is reversed relative to the heavier odd- $A$  Bi isotopes, with the intruder-based  $1/2^+$  configuration becoming the ground, similar to the lightest At nuclides.

DOI: 10.1103/PhysRevLett.127.202501

Proton radioactivity, where the atomic nucleus is energetically unstable to the spontaneous emission of a proton, is a key, and often the only, source of nuclear structure and mass-landscape information at, and beyond, the proton drip line [1–7]. The location of the proton drip line, and the structure of the exotic nuclei that lie on it, also constrains the path of nucleosynthesis and the termination of the  $r$  $p$  process in explosive astrophysical environments, such as x-ray bursts, see, e.g., Refs. [7–9].

The phenomenon of proton radioactivity from the ground state (gs) has been experimentally observed in the most neutron-deficient isotopes of all odd- $Z$  nuclides with  $53 \leq Z \leq 83$ , see Ref. [2] and references therein, with promethium ( $Z = 61$ ) being the only exception. Proton decay is a quantum-tunneling phenomenon, but, in contrast to  $\alpha$  decay, which requires the consideration of the formation of an  $\alpha$  particle on the surface of the nucleus, the pre-existence of protons within the nucleus allows for its simpler theoretical treatment [10,11]. Furthermore, due to its strong dependence on the proton's energy and orbital

angular momentum, the proton decay rate is often used to assign specific configurations to the parent nuclide. Indeed, as shown in, e.g., Ref. [12], several theoretical approaches, applied to *spherical* proton emitters ( $Z = 69\text{--}81$ ), provide a fair description of their half-lives and spectroscopic factors (where the latter defines overlap between the wave functions of the parent and daughter states plus one proton), without much sensitivity to the specific choice of model parameters. The situation is more complex for both moderately and strongly deformed proton emitters with  $Z = 53\text{--}67$ . In such cases, the proton orbital angular momentum  $l_p$  is no longer conserved, and different components can contribute to the decay rate [13], producing major changes in the (predicted) half-life compared to spherical calculations [12–15]. So far, only one case of proton decay has been measured involving a daughter nucleus with a major shell closure,  $^{185}\text{Bi}$  ( $Z = 83$ )  $\rightarrow$   $^{184}\text{Pb}$  ( $Z = 82$ ) the heaviest known proton emitter [2], which could provide a fundamental benchmark for modeling the proton decay process. However, this  $l_p = 0$  decay has

hitherto been found to be significantly hindered [16–18] compared to spherical calculations and the origin of this hindrance was not yet understood.

The  $^{185}\text{Bi}$  nuclide was first observed in 1996 at the fragment mass analyzer (FMA) at Argonne National Laboratory [16], where seven protons and one  $\alpha$ -decay event were recorded. In the following decade, improved statistics were obtained in a further FMA study [17] (23 protons and 5  $\alpha$  decays) and at the velocity filter SHIP, GSI [18] (214 protons and 27  $\alpha$  decays). In all of these studies, only a *single* particle-decaying state with  $T_{1/2} = 60(3) \mu\text{s}$ , assigned as  $I^\pi = 1/2^+$ , was observed, decaying predominantly via a 90(2)% proton-emission branch to the  $^{184}\text{Pb}$  gs [19], with a 10(2)%  $\alpha$ -decay branch to the spherical  $1/2^+$  gs of  $^{181}\text{Tl}$  [20]; the branching ratios are taken from [18].

The presently known decay properties of  $^{185}\text{Bi}$  display a number of puzzling features. First, no  $9/2^-$  level has so far been observed, which is in contrast to all odd- $A$  isotopes  $^{187-209}\text{Bi}$ , with  $9/2^- [\pi(h_{9/2})^1]$  ground states. In addition, weakly oblate  $1/2^+ \pi(h_{9/2})^2 \otimes (s_{1/2})^{-1}$  intruder states have been identified in  $^{187-209}\text{Bi}$  [21,22].

Second, as shown in Table 1 of Ref. [18], using the known proton decay energy  $E_p = 1598(16) \text{ keV}$  [17] and spherical WKB tunneling probability calculations, the calculated  $l_p = 0$  decay half-life is  $T_{\frac{1}{2},\text{WKB}} = 1.7 \mu\text{s}$ . This results in a low experimental spectroscopic factor  $T_{\frac{1}{2},\text{WKB}}/T_{\frac{1}{2},\text{exp}} = 0.025(2)$ , which is comparable to the experimental values deduced in Refs. [5,16]. To account for this strong hindrance, the previous studies suggested a deformed configuration for the  $1/2^+$  gs in  $^{185}\text{Bi}$ , which would inhibit the decay to the predominantly spherical  $0^+$  gs of  $^{184}\text{Pb}$ , albeit different signs of deformation were proposed—an oblate shape in the FMA works [16,17] and a prolate one in the SHIP study [18]. Mixing of the excited intruder  $0_2^+$  level, at 570 keV, and the gs,  $0_{\text{gs}}^+$ , in the  $^{184}\text{Pb}$  daughter was invoked to account for this hindrance [16,17].

Third, previous studies noted that the  $\text{gs} \rightarrow \text{gs}$ ,  $1/2^+ \rightarrow 1/2^+$ ,  $\alpha$  decay of  $^{185}\text{Bi} \rightarrow ^{181}\text{Tl}$  was hindered by a factor 14(3) [18]. This is in stark contrast to the unhindered  $1/2^+ \rightarrow 1/2^+$  and  $9/2^- \rightarrow 9/2^-$   $\alpha$  decays observed between  $^{187-195}\text{Bi}$  and their Tl daughters, as summarized in, e.g., Fig. 4(b) of Ref. [18]. This hindrance was interpreted as possible evidence for a change in the configuration of the  $1/2^+$  level in  $^{185}\text{Bi}$  with respect to the  $1/2^+$  states in the heavier, odd- $A$  Bi isotopes. This was indirectly supported by extensive potential-energy surface (PES) and particle-rotor calculations for odd- $A$   $^{185-195}\text{Bi}$  isotopes presented in Figs. 6 and 7 of Ref. [18].

It is also important to note that the study of Poli *et al.* [17] was the first to question whether the  $1/2^+$  state may lie below the spherical  $h_{9/2}$  orbital and become the gs in  $^{185}\text{Bi}$ . This suggestion is in line with a well-documented experimental downward trend in the excitation energy of  $1/2^+$  states in the odd- $A$  Bi isotopes approaching the neutron

midshell at  $N = 104$  ( $^{187}\text{Bi}$ ). However, no experimental confirmation yet existed for the swapping of the  $1/2^+$  and  $9/2^-$  states in  $^{185}\text{Bi}$ , as the  $9/2^-$  state had yet to be observed. Such a switch has been experimentally observed in the lightest odd- $A$  isotopes  $^{191-193}\text{At}$  ( $Z = 85$ ) [23,24], where the  $1/2^+$  intruder level becomes the gs.

Therefore, one of the main goals of this Letter was to search for excited states above the presumed  $1/2^+$  gs of  $^{185}\text{Bi}$ , which could decay via  $\gamma$ -ray transitions or particle emission. This is a challenging task due to the difficulty in producing a sufficient number of  $^{185}\text{Bi}$  nuclei, in a suitable reaction, and separating them from other, more strongly produced, reaction products.

Nevertheless, as we can report in this Letter, by performing two complementary experiments exploiting an advanced fully digital focal plane detection setup and pulse-shape analysis, at both the FMA [25] and the Argonne gas-filled analyzer (AGFA) [26], it was possible to identify a  $58(2)\text{-}\mu\text{s}$   $\gamma$ -decaying isomeric state in  $^{185}\text{Bi}$ , which is most probably a ( $7/2^-$ ) or ( $9/2^-$ ) level. In doing so, it is demonstrated that the previously known  $60(3)\text{-}\mu\text{s}$  half-life should be attributed to this new excited state, while a much shorter half-life of  $2.8_{-1.0}^{+2.3} \mu\text{s}$  is measured for the  $1/2^+$  gs. This new information confirms the inverting of high- and low-spin states in  $^{185}\text{Bi}$  and brings the proton spectroscopic factor and reduced  $\alpha$ -decay width in line with the systematics of the heavier odd- $A$  Bi isotopes and, consequently, leads to a better understanding of the configuration of  $^{185}\text{Bi}$ .

The  $^{185}\text{Bi}$  nuclei were produced via the  $^{95}\text{Mo}(^{93}\text{Nb}, 3n)$  fusion-evaporation reaction, at a beam energy of 424 MeV with  $\sim 780\text{-}\mu\text{g}/\text{cm}^2$ -thick  $^{95}\text{Mo}$  targets. In the first experiment, which lasted  $\sim 105$  h, with an average beam intensity of 20 pA, recoiling reaction products were dispersed according to their mass-to-charge ratio using the FMA [25] and then passed through a parallel-grid avalanche counter and a transmission ionization chamber before being implanted into a  $\sim 100\text{-}\mu\text{m}$ -thick,  $64 \times 64 \text{ mm}^2$ ,  $160 \times 160$  strip double-sided silicon strip detector (DSSD). By employing spatial and temporal correlations, particle decay events from  $^{185}\text{Bi}$  could be cleanly identified, for events where the decay time is longer than  $10 \mu\text{s}$ , as shown in Fig. 1. A total of 216  $^{185}\text{Bi}$  protons and 19  $\alpha$ -decay events were observed with a decay half-life of  $58(3) \mu\text{s}$ , in agreement with previous work [16–18], but, as we show below, the data obtained here require a new interpretation of the  $^{185}\text{Bi}$  decay properties. The focal plane setup was augmented by installing the Argonne X-Array [27], which consisted of five clover high-purity germanium detectors in a closely packed geometry, for measuring delayed and prompt  $\gamma$  rays correlated with decay events. The data from each of the channels were recorded independently, and each event was time stamped with a 100 MHz clock.

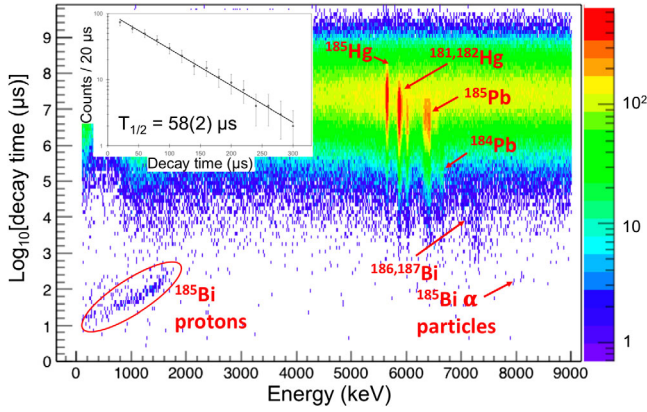


FIG. 1. The logarithm of the time difference between a recoil implantation and a subsequent decay event occurring in the same pixel of the DSSD as a function of the energy deposited by the decay event, from the FMA experiment; see text for details. Some groups are labeled with the isotopes they originate from. The slope in proton locus is due to the event being piled up with the recoil signal, see Fig. 1 of the Supplemental Material [28] for a pileup corrected spectrum. The inset shows the proton decay curve obtained by combining the FMA and AGFA datasets.

In order to benchmark the setup,  $\alpha$ - $\gamma$  coincidences for the strongly produced  $^{185}\text{Pb}$  isotope [ $T_{1/2} = 6.3(4)$  s] were investigated. The resulting  $\gamma$ -ray spectra are clean and are in excellent agreement with earlier work [29], giving confidence in the analysis procedures and in the discussion below. These data were also used to improve the X-Array energy calibration at low energies, using Hg x rays observed following the  $\alpha$  decay of Pb isotopes and as a timing reference for the prompt decay- $\gamma$  events.

In order to search for  $\gamma$  rays correlated with  $^{185}\text{Bi}$  events at the focal plane, recoil- $\gamma$ -decay event chains were studied. The resulting  $\gamma$ -ray spectrum, gated by  $^{185}\text{Bi}$  proton or  $\alpha$  decays within 300  $\mu\text{s}$  of the recoil implantation, is shown in Fig. 2. Fifteen events are observed in an otherwise extremely clean spectrum, including a clear peak, consisting of six

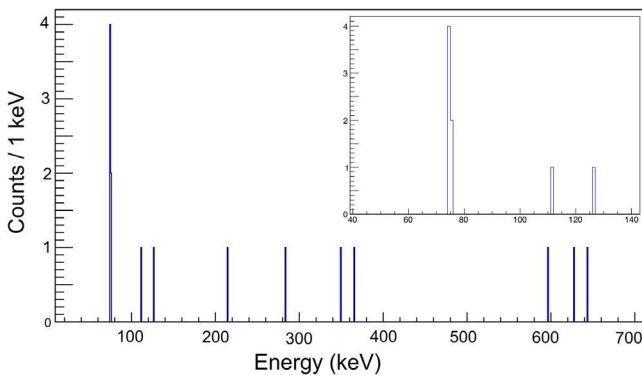


FIG. 2. The  $\gamma$ -ray spectrum obtained with the X-Array for events where an implant is followed by either a proton or  $\alpha$  decay from  $^{185}\text{Bi}$ , in the same pixel of the DSSD, within 300  $\mu\text{s}$  of the recoil. The inset shows the same spectrum enlarged in the low-energy region of interest.

counts, at an energy of 74 keV. This transition represents the first evidence of decay from an isomeric state in  $^{185}\text{Bi}$  and, indeed, the first knowledge on any excited state in this nucleus.

The energy and timing information of these 74-keV events is given in Table I, four of these were followed by a proton and one by the emission of an  $\alpha$  particle. Based on a maximum likelihood analysis of the five  $\gamma$ -ray events, a lifetime of 82(33)  $\mu\text{s}$  [ $T_{1/2} = 57(23)$   $\mu\text{s}$ ] is determined for the isomeric level and  $4.0^{+3.3}_{-1.4}$   $\mu\text{s}$  ( $T_{1/2} = 2.8^{+2.3}_{-1.0}$   $\mu\text{s}$ ) for the particle-emitting gs. Importantly, one of these  $\gamma$  rays is observed in prompt coincidence, within 20 ns, with another  $\gamma$  ray at 75.0 keV; this pair will be discussed further later in the text.

We suggest that the 74-keV transition is most likely a  $\gamma$  ray as it is distinct from the Bi  $K_{\alpha 1}$  x-ray energy (77.1 keV [30]), while  $K_{\alpha 2}$  x rays (74.8 keV in Bi [30]) are less intense (60% of the  $K_{\alpha 1}$  intensity). However, with the present statistics, we cannot completely rule out the possibility that a subset of the observed 74-keV  $\gamma$  rays corresponds to Bi  $K_{\alpha 2}$  x rays from converted transition(s). For example, one of the  $\gamma$  rays in the coincident event could be a 74-keV transition, while the second is a Bi  $K$  x ray from a coincident, converted one. Therefore, we suggest that the observation of delayed  $\gamma$  rays should be interpreted as the deexcitation of a long-lived isomeric state in  $^{185}\text{Bi}$  [ $T_{1/2} = 57(23)$   $\mu\text{s}$ ], which is responsible for the previously reported ground-state half-life of 60(3)  $\mu\text{s}$  [18].

In order to confirm the short-lived nature of the gs, a follow-up experiment was performed with AGFA, with the aim of observing possible fast protons events where the isomeric state is bypassed. The use of a symmetric reaction presented a challenge in suppressing the beam at the AGFA focal plane and, thus, the beam intensity was limited to  $\sim 10$  pA. It also prohibited the use of the X-Array due to the large random rate. However, despite twice lower beam current than was used in the FMA experiment, the larger transport efficiency of AGFA resulted in a  $\sim 50\%$  higher  $^{185}\text{Bi}$  rate (139 protons and 11  $\alpha$  particles in  $\sim 92$  h,

TABLE I. Energy and timing information for events in the 74-keV peak. The  $\gamma$ -decay times are determined relative to the prompt peak, as shown in Fig. 2 of the Supplemental Material [28], while the recoil- $\gamma$  time is determined indirectly from the measured particle decay times.

| Event          | $E_{\gamma}$ (keV) | Rec- $\gamma$ time ( $\mu\text{s}$ ) | $\gamma$ - $p$ time ( $\mu\text{s}$ )      |
|----------------|--------------------|--------------------------------------|--|
| 1              | 75.1               | 56.86                                | 4.68                                       |
| 2 <sup>a</sup> | 74.1, 75.0         | 10.85                                | 3.67                                       |
| 3              | 74.3               | 56.88                                | 3.66                                       |
| 4              | 74.0               | 80.19                                | 4.34                                       |
| Event          | $E_{\gamma}$ (keV) | Rec- $\gamma$ time ( $\mu\text{s}$ ) | $\gamma$ - $\alpha$ time ( $\mu\text{s}$ ) |
| 5              | 74.3               | 209.24                               | 4.02                                       |

<sup>a</sup>Coincident event, the 74.1- and 75.0-keV  $\gamma$  rays are separated by 20 ns.

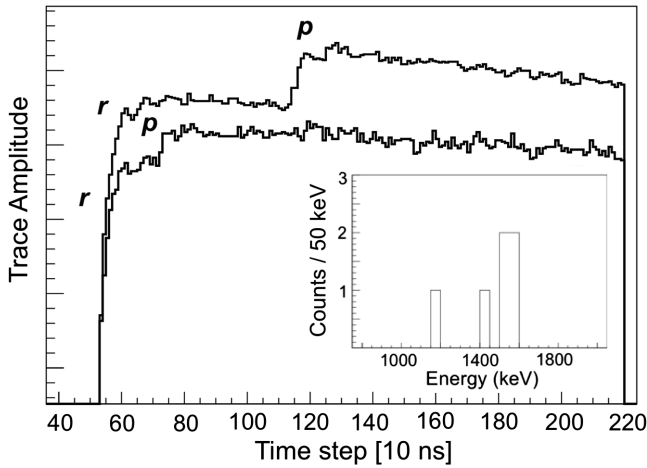


FIG. 3. Example waveforms for recoil ( $r$ )-proton ( $p$ ) decay events, where the recoil is followed by a  $^{184}\text{Pb}$   $\alpha$  decay in the same DSSD pixel. The inset shows the energy spectrum obtained by extracting the proton-decay energies from the six pileup waveforms. A matrix of  $^{185}\text{Bi}(p)$ - $^{184}\text{Pb}(\alpha)$  decay events is shown in Fig. 4 of the Supplemental Material [28].

see Fig. 3 of the Supplemental Material [28]). Combining the recoil-particle decay data from both experiments yields a  $^{185}\text{Bi}$  half-life of  $58(2) \mu\text{s}$ , as shown in the inset of Fig. 1, which is herewith shown to belong to the newly identified isomeric level.

Information on  $< 10\text{-}\mu\text{s}$  particle decays can be obtained by investigating pileup waveforms. In the AGFA experiment, waveforms were read out spanning  $1.7 \mu\text{s}$  and starting  $0.5 \mu\text{s}$  before the leading edge of the signal; the high event rate at the focal plane prevented the recording of longer waveforms.

To focus the pileup waveform analysis on candidate  $^{185}\text{Bi}$  fast proton events, the waveforms for chains of events where a recoil was followed by an  $\alpha$  decay from the daughter nucleus  $^{184}\text{Pb}$  in the same DSSD pixel were investigated. The candidate waveforms had to yield consistent signals from the front and back of the DSSD.

In total, six waveforms were observed within the  $1.7\text{-}\mu\text{s}$ -long window with an extracted proton energy within  $\sim 500$  keV of the known  $^{185}\text{Bi}$  proton energy of  $1598(16)$  keV [17], see Fig. 3 for examples of fast proton waveforms and the extracted energy spectrum. An upper limit of only one event would be expected, within the  $1.7\text{-}\mu\text{s}$  window, assuming a  $58(2)\text{-}\mu\text{s}$  half-life (this upper limit is determined from an analysis of the recoil- $^{185}\text{Bi}$  proton- $^{184}\text{Pb}$   $\alpha$ -decay event chains). Decay times of  $0.20$ ,  $0.30$ ,  $0.55$ ,  $0.65$ ,  $1.50$ , and  $1.60 \mu\text{s}$  were obtained from the waveforms, which is consistent with the short half-life deduced from the FMA data.

The identification of a  $58\text{-}\mu\text{s}$  isomeric state and the new half-life of  $2.8_{-1.0}^{+2.3} \mu\text{s}$  for the proton-emitting gs of  $^{185}\text{Bi}$  has several implications for understanding past work and for proposing a new decay scheme.

The ground-state half-life fits well with the theoretical value of  $1.7 \mu\text{s}$ , determined from spherical WKB calculations for  $l_p = 0$  decay performed for  $^{185}\text{Bi}$  (see Table 1 of Ref. [18]), giving an experimental spectroscopic factor of  $\sim 0.6$ , close to unity. Such a value signifies unhindered proton decay from  $^{185}\text{Bi}$  to the  $0^+$  gs of  $^{184}\text{Pb}$  and firmly establishes the  $I^\pi = 1/2^+$  assignment for the gs.

In the previous studies [16–18], a low spectroscopic factor of  $0.025$  was deduced, based on a  $\sim 60\text{-}\mu\text{s}$  half-life value, which demanded a strong difference between the parent and daughter configurations. In contrast, our new, much larger, spectroscopic factor demonstrates the closer matching in the wave functions of the parent and daughter systems. The PES calculations, presented in Figs. 7(a) and 8 of Ref. [18], clearly indicate the possible presence of several low-lying  $1/2^+$  states in  $^{185}\text{Bi}$ , with different deformations, including a mixed oblate-prolate configuration with  $\beta_2 \sim 0.15$  and a strongly prolate deformed one with  $\beta_2 \sim 0.29$ . The calculations predict that the latter becomes the gs. However, this configuration has to be ruled out due to its  $i_{13/2}$  nature (leading to  $l_p = 6$  decay), which would result in very large hindrance, contrary to the deduced spectroscopic factor close to unity. Therefore, our data establish that the gs of  $^{185}\text{Bi}$  originates from a mixed prolate-oblate configuration based on the  $s_{1/2}$  orbital, with a relatively small deformation of  $\beta_2 \sim 0.15$ . We refer the reader to Sec. IV F of [18] for a discussion of this state's mixing properties. The unhindered character of the proton decay is explained by the mixed nature of the  $^{184}\text{Pb}$  daughter gs. This was demonstrated in [19] and is due to the presence of a, presumably, prolate-deformed excited  $0^+$  state in  $^{184}\text{Pb}$ , see Fig. 4. We also note that the shape change does not hinder the  $^{185}\text{Bi}$  gs to spherical  $^{181}\text{Tl}$  gs  $\alpha$  decay. The newly determined reduced width value,  $\delta_\alpha^2 = 64_{-21}^{+61}$  keV, now fits well with the systematics of unhindered  $1/2^+ \rightarrow 1/2^+$   $\alpha$  decays observed between deformed intruder states in  $^{187\text{--}195}\text{Bi}$  and spherical gs in the Tl daughters, see Fig. 4 of [18].

The data also enable relative populations of  $\sim 80\%$  and  $\sim 20\%$  for the isomeric level and the gs, respectively, to be estimated, for this reaction. Higher-spin states are generally observed to be produced more strongly, following heavy-ion fusion-evaporation reactions, for heavier isotopes in this region [29,31]. The larger population of the  $58\text{-}\mu\text{s}$  isomeric level, therefore, suggests that it is a high-spin state.

To assist with the interpretation of the isomeric state, it is useful to examine the systematics for  $1/2^+$ ,  $7/2^-$  and  $9/2^-$  levels in the neutron-deficient odd- $A$  Bi and At isotopes. Namely, the  $^{187\text{--}209}\text{Bi}$  and  $^{197\text{--}211}\text{At}$  nuclides have  $9/2^-$  [ $\pi h_{9/2}$ ] ground states and excited intruder  $1/2^+$  configurations. However, the  $1/2^+$  level becomes the gs in  $^{191,193,195}\text{At}$  with a  $7/2^-$  first excited state [23,24].

In  $^{187,189,191,193}\text{Bi}$ , several low-lying states have been identified [32] and the most relevant for this study, the

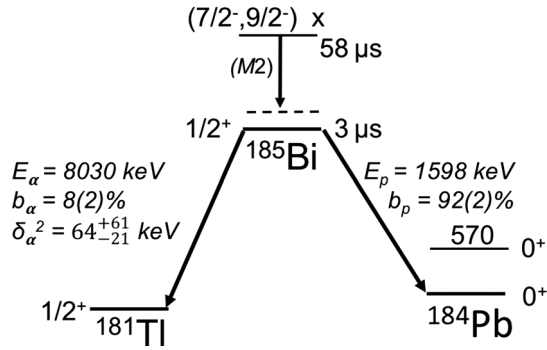


FIG. 4. The proposed decay pattern of  $^{185}\text{Bi}$ . The excitation energy of the  $58\text{-}\mu\text{s}$  isomeric state is not yet known. The most likely spin-parity assignment is  $7/2^-$  or  $9/2^-$ , with different decay paths toward the  $3\text{-}\mu\text{s}$   $1/2^+$  gs, depending on the specific assignment; see text for details. The nature of the intermediate level(s), shown with a dashed line, is discussed in the text. The branching ratios  $b_p$  and  $b_\alpha$  are determined in the present Letter. The proton and  $\alpha$  decay energy of  $^{185}\text{Bi}$ , and excitation energy of the  $0_2^+$  state in  $^{184}\text{Pb}$  are taken from [16] and [32], respectively.

$9/2^-$ ,  $1/2^+$ ,  $7/2^-$ , and  $13/2^+$  levels, are presented in Fig. 5 of the Supplemental Material [28]. The  $1/2^+$ ,  $7/2^-$ , and  $13/2^+$  states show a strong downward trend in excitation energy, relative to the gs, approaching the neutron midshell at  $N = 104$  ( $^{187}\text{Bi}$ ). In  $^{187}\text{Bi}$ , these four states are actually the lowest-lying single-particle proton levels, with all of them being observed within 250 keV. Based on these systematics, and by analogy with the At data mentioned above, it is plausible to expect both  $7/2^-$  and  $9/2^-$  levels close to the  $1/2^+$  gs.

In order to reconcile the small number of observed  $\gamma$  rays, accounting for an X-Array efficiency of  $\sim 25\%$  at 74 keV, with the number of protons registered in the FMA experiment, it is necessary that the transition energy is below the Bi  $K$ -shell binding energy of 91 keV [33]. Consequently,  $L$ -shell conversion dominates, producing x rays ( $L_{\alpha 1} = 10.8 \text{ keV}$ ) that are below the energy threshold of the X-Array. Weisskopf estimates then indicate that an isomeric state with a half-life of  $58 \mu\text{s}$  can only be explained by an  $M2$  decay. Indeed, for a  $\gamma$  ray with an energy of 74 keV, the calculated half-life is  $\sim 15 \mu\text{s}$ . In contrast, an  $E3$  decay, of comparable energy, would have a half-life that is 4 orders of magnitude longer and an  $E2$  transition would have to be unusually hindered to account for the experimentally observed half-life.

Based on these arguments, we propose the new decay scheme shown in Fig. 4, where an excited  $7/2^-$  or  $9/2^-$  level is situated above the  $1/2^+$  gs in  $^{185}\text{Bi}$  and decays via an  $M2$  transition. The observation of a  $\gamma$ - $\gamma$  coincident event (event 2 in Table I) means that both scenarios require one or possibly two intermediate states, as shown schematically in Fig. 4. We note that low-lying  $3/2^+$  and  $5/2^+$  excited levels, built on top of the  $1/2^+$  intruder state, have already been observed in  $^{191,193}\text{Bi}$  [34,35]. While a strongly

coupled rotational band is observed in  $^{193}\text{Bi}$  [34], the situation in  $^{191}\text{Bi}$  is more complex with a  $3/2^+$  and two  $5/2^+$  levels observed within 370 keV of the  $1/2^+$  state [35]. This suggests that, moving toward  $^{185}\text{Bi}$ , the low-lying level structure becomes more complex again with a number of low-spin states ( $1/2^+$ ,  $3/2^+$ , and  $5/2^+$ ) expected at very low excitation energies. This is supported by the theoretical calculations presented in Fig. 8 of Ref. [18]. The most plausible scenarios, therefore, are that, in the event of a  $7/2^-$  isomeric level, the decay proceeds via an  $M2$  transition toward a low-lying  $3/2^+$  state, followed by an  $M1$  decay to  $1/2^+$  gs, whereas for a  $9/2^-$  isomer the  $M2$  decay is to a  $5/2^+$  level, followed by a single  $\gamma$  ray or by a cascade to the gs.

In summary, in complementary experiments with the FMA and AGFA, a long-lived,  $58\text{-}\mu\text{s}$  isomeric state in  $^{185}\text{Bi}$  has been identified, which is likely a  $7/2^-$  or  $9/2^-$  level, which decays via a delayed cascade of  $\gamma$  rays toward the newly established  $2.8_{-1.0}^{+2.3}\text{-}\mu\text{s}$  gs. This half-life is consistent with  $l_p = 0$  decay from an  $s_{1/2}$  orbital and, consequently, both the proton and  $\alpha$  decay of  $^{185}\text{Bi}$  are now shown to be unhindered.

These results clearly motivate further dedicated decay spectroscopy studies of  $^{185}\text{Bi}$ , in order to examine the  $\gamma$  decay of the isomeric level in detail. Such experiments will require intense beams and would, ideally, make use of Ge detectors at the focal plane of a separator that are highly sensitive at low energies; see, for example, Ref. [36]. In addition, it will be important to perform in-beam spectroscopy, employing the recoil-decay tagging technique (e.g., [37]), in order to search for excited levels on top of states observed in this Letter, which might allow for a better determination of their underlying configuration.

This work was supported by the U.S. Department of Energy, Office of Nuclear Physics, under Award No. DE-AC02-06CH11357 and Grants No. DE-FG02-94ER41041 (UNC) and No. DE-FG02-97ER41033 (TUNL). This research used resources of ANL's ATLAS facility, which is a DOE Office of Science User Facility. United Kingdom personal are grateful for financial support from the STFC.

\*Present address: Department of Physics, University of Jyväskylä, P.O. Box 35, FI-40014 Finland.

†Present address: Università degli Studi di Milano and INFN, Via Celoria 16, I-20133 Milano, Italy.

- [1] B. Blank and M. J. G. Borge, *Prog. Part. Nucl. Phys.* **60**, 403 (2008).
- [2] M. Pfützner, M. Karny, L. V. Grigorenko, and K. Riisager, *Rev. Mod. Phys.* **84**, 567 (2012).
- [3] P. J. Woods, *Nature (London)* **381**, 25 (1996).
- [4] C. N. Davids *et al.*, *Phys. Rev. C* **55**, 2255 (1997).
- [5] G. D. Poli *et al.*, *Phys. Rev. C* **59**, R2979(R) (1999).
- [6] A. N. Andreyev *et al.*, *Phys. Rev. C* **80**, 024302 (2009).

- [7] P. J. Woods and C. N. Davids, *Annu. Rev. Nucl. Part. Sci.* **47**, 541 (1997).
- [8] K. Auranen *et al.*, *Phys. Lett. B* **792**, 187 (2019).
- [9] P. Siwach, P. Arumugam, S. Modi, L. S. Ferreira, and E. Maglione, *Phys. Rev. C* **103**, L031303 (2021).
- [10] C. Qi, R. Liotta, and R. Wyss, *Prog. Part. Nucl. Phys.* **105**, 214 (2019).
- [11] C. Qi, R. Liotta, and R. Wyss, *Phys. Lett. B* **818**, 136373 (2021).
- [12] S. Åberg, P. B. Semmes, and W. Nazarewicz, *Phys. Rev. C* **56**, 1762 (1997).
- [13] L. S. Ferreira and E. Maglione, *Phys. Rev. Lett.* **86**, 1721 (2001).
- [14] A. Gillitzer, T. Faestermann, K. Hartel, P. Kienle, and E. Noite, *Z. Phys. A* **326**, 107 (1987).
- [15] H. Esbensen and C. N. Davids, *Phys. Rev. C* **63**, 014315 (2000).
- [16] C. N. Davids *et al.*, *Phys. Rev. Lett.* **76**, 592 (1996).
- [17] G. L. Poli *et al.*, *Phys. Rev. C* **63**, 044304 (2001).
- [18] A. N. Andreyev *et al.*, *Phys. Rev. C* **69**, 054308 (2004).
- [19] H. De Witte *et al.*, *Phys. Rev. Lett.* **98**, 112502 (2007).
- [20] A. E. Barzakh *et al.*, *Phys. Rev. C* **95**, 014324 (2017).
- [21] E. Coenen, K. Deneffe, M. Huyse, P. Van Duppen, and J. L. Wood, *Phys. Rev. Lett.* **54**, 1783 (1985).
- [22] J. C. Batchelder *et al.*, *Eur. Phys. J. A* **5**, 49 (1999).
- [23] H. Kettunen *et al.*, *Eur. Phys. J. A* **17**, 537 (2003).
- [24] H. Kettunen *et al.*, *Eur. Phys. J. A* **16**, 457 (2003).
- [25] C. N. Davids and J. D. Larson, *Nucl. Instrum. Methods Phys. Res., Sect. B* **40–41**, 1224 (1989).
- [26] B. B. Back *et al.*, *EPJ Web Conf.* **163**, 00003 (2017).
- [27] A. J. Mitchell *et al.*, *Nucl. Instrum. Methods Phys. Res., Sect. A* **763**, 232 (2014).
- [28] See Supplemental Material at <http://link.aps.org/supplemental/10.1103/PhysRevLett.127.202501> for additional information from both the FMA and AGFA experiments.
- [29] A. N. Andreyev *et al.*, *Eur. Phys. J. A* **14**, 63 (2003).
- [30] A. C. Thompson *et al.*, *X-Ray Data Booklet*, 2nd ed. (Lawrence Berkeley National Laboratory, Berkeley, 2001).
- [31] A. N. Andreyev *et al.*, *Eur. Phys. J. A* **18**, 39 (2003).
- [32] F. G. Kondev, M. Wang, W. Huang, S. Naimi, and G. Audi, *Chin. Phys. C* **45**, 030001 (2021).
- [33] T. Kibedi, T. Burrows, M. Trzhaskovskaya, P. Davidson, and C. N. Jr, *Nucl. Instrum. Methods Phys. Res., Sect. A* **589**, 202 (2008).
- [34] A. Herzan *et al.*, *Phys. Rev. C* **92**, 044310 (2015).
- [35] M. Nyman *et al.*, *Eur. Phys. J. A* **51**, 31 (2015).
- [36] S. A. Gillespie *et al.*, *Phys. Rev. C* **103**, 044307 (2021).
- [37] D. Seweryniak *et al.*, *Phys. Rev. Lett.* **99**, 082502 (2007).